Solid State Ionics 244 (2013) 5–16

Contents lists available at SciVerse ScienceDirect

Solid State Ionics

journal homepage: www.elsevier.com/locate/ssi

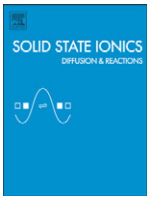

Conductive AFM and chemical analysis of highly conductive paths in DC degraded PZT with Ag/Pd electrodes

L. Andrejs [a], H. Oßmer [a], G. Friedbacher [b], J. Bernardi [c], A. Limbeck [b], J. Fleig [a,*]

[a] *Christian Doppler Laboratory for Ferroic Materials, Institute of Chemical Technologies and Analytics, Vienna University of Technology, 1060 Vienna, Austria*
[b] *Institute of Chemical Technologies and Analytics, Vienna University of Technology, 1060 Vienna, Austria*
[c] *University Service Center for Transmission Electron Microscopy, Vienna University of Technology, 1040 Vienna, Austria*

ARTICLE INFO

Article history:
Received 20 December 2012
Received in revised form 16 April 2013
Accepted 22 April 2013
Available online 31 May 2013

Keywords:
Degradation
Silver filaments
Grain boundaries
C-AFM
PZT

ABSTRACT

DC degraded PZT layers were studied by means of energy dispersive X-ray spectroscopy (EDX), laser ablation-inductively coupled plasma-mass spectrometry (LA-ICP-MS), transmission electron microscopy (TEM), scanning electron microscopy (SEM) and conductive atomic force microscopy (C-AFM). It is shown that mainly silver originating from the anode is massively redistributed on/in the PZT during voltage load. Highly conductive silver paths/filaments are strongly localized to grain boundaries in the bulk of the PZT layers and unambiguously identified as responsible for metal-like connection between anode and cathode. Formation of these paths starts close to the anode. This indicates the existence of a novel mode of resistance degradation without impact of humidity. A corresponding mechanism based on voltage induced oversaturation of PZT grains with silver and non-conventional electrochemical formation of anodic silver filaments is suggested.

1. Introduction

Mechanisms of resistance degradation in donor-doped perovskite-type electroceramics are rarely discussed in literature. This is partly because typical materials of this group such as donor-doped $SrTiO_3$ or $BaTiO_3$ are effectively protected against an important degradation mechanism occurring at enhanced temperatures, namely oxygen vacancy stoichiometry polarization between (ionically) blocking electrodes: Owing to the strongly suppressed oxygen vacancy concentration compared to acceptor-doped perovskites [1–3], hardly any change of electronic charge carrier conductivity is induced by oxygen vacancy motion upon DC load. Lead-based perovskites with high oxygen vacancy concentrations (e.g. PMN-PT [4]) were shown to suffer from degradation by stoichiometry polarization and oxygen vacancy related degradation was even discussed for donor-doped lead zirconate titanate (PZT [5,6]). However, minor importance of this degradation mode was found in Ref. [6].

On the other hand, it was recently shown by measurements at temperatures above 420 °C that a cation related process in donor-doped PZT with Ag/Pd electrodes may be responsible for massive resistance losses under DC load [7,8]. A conventional electrodeposition process with cathodic Ag dendrite formation upon load could be excluded as the cause of the resistance degradation; the latter is only found under high humidity and moderate temperatures [9] or e.g. in electrochemical metallization cells using a silver electrode and a silver ion conducting solid electrolyte [10]. As a side effect, this degradation is accompanied by formation of silver droplets on the surface, starting close to the anode and then proceeding towards the cathode. A novel resistance degradation model for donor-doped PZT with silver rich electrodes was therefore suggested [8]. It clearly differs from models discussed in the context of possibly reversed growth of filaments in resistive switching memory devices [11,12] (see also comments on Ref. [12] in Refs. [13,14]). Our model is based on DC voltage driven formation of metal-like conductive paths in the bulk of PZT close to the anode and further growth of these paths (most probably along grain boundaries) through the ceramics to the cathode. However, a number of questions regarding this novel degradation mechanism have remained open. For example, a final proof of conducting filament formation in grain boundaries as well as detailed information on their growth mode and growth direction is missing.

In this contribution, we present experimental results in order to further clarify and specify the degradation mechanism of PZT with silver rich electrodes in the absence of humidity. An extensive study was performed focusing on localization and visualization of conducting paths in the PZT layers by means of conductive atomic force microscopy (C-AFM). Additionally, appearance and properties of surface precipitates were studied in detail using C-AFM, scanning electron microscopy (SEM) and energy dispersive X-ray spectroscopy (EDX). The latter methods together with transmission electron microscopy (TEM) and laser ablation-inductively coupled plasma-mass spectrometry (LA-ICP-MS) were also employed for the analysis of chemical

---

[*] Corresponding author at: Christian Doppler Laboratory for Ferroic Materials, Institute of Chemical Technologies and Analytics, Vienna University of Technology, Getreidemarkt 9/164-EC, 1060 Vienna, Austria. Tel.: +43 1 58801 158 00; fax: +43 1 58801 15899.
E-mail address: j.fleig@tuwien.ac.at (J. Fleig).

0167-2738/$ – see front matter © 2013 Elsevier B.V. All rights reserved.
http://dx.doi.org/10.1016/j.ssi.2013.04.020

changes in the bulk of the degraded layers. The experimental results are used to detail the resistance degradation model and to provide mechanistic interpretation.

2. Experimental

2.1. PZT material and DC resistance degradation

In accordance with preceding papers [7,8], the measurements were carried out on square-shaped samples (ca. 7 × 7 × 1.5 mm; Fig. 1) prepared from 1.5% neodymium (donor) doped PZT multilayer actuator stacks (Epcos OHG A Member of TDK-EPC Corporation, Deutschlandsberg, Austria). The stacks consist of polycrystalline PZT layers ($Pb(Zr_{0.52}Ti_{0.48})O_3$) alternating with silver/palladium inner electrodes. Stacks with two slightly different electrode compositions (Ag/Pd ratios of 80/20 and 75/25) were employed. All features relevant in this study (current fluctuations, massive resistance losses and formation of surface precipitates during long-time DC load) were identical for both types of electrodes (see also Ref. [8]). The different samples are denoted as PZT-80/20 and PZT-75/25 throughout this paper. For resistance degradation a DC voltage of 5 to 10 V was applied to individual, virgin PZT layers of ca. 80 μm thickness (electric field from 0.625 to 1.25 kV/cm) at 390–520 °C set temperature (nominal temperature of the heating stage, cf. [7]). This led to the formation of differently shaped features (here called precipitates) on the PZT surface quite soon after applying the field stress and later to a massive resistance degradation in the ceramic layers after a few tens of minutes to a few hours (resistance drop by 3 to 4 orders of magnitude). Tests in wet ambient atmosphere and dry synthetic air did not reveal any difference, thus indicating irrelevance of water in all processes discussed here [15]. In order to enable further investigations of the degraded layers, the samples were quenched to room temperature where these layers exhibited high, metal-like conductivity (ca. 10^1–10^2 Ω [7]). More details on the sample preparation and the experimental procedures are given in references [7,8].

2.2. Electron microscopy

Virgin as well as degraded layers were investigated using a scanning electron microscope (FEI Quanta 200, FEI, USA) equipped with an energy dispersive X-ray spectrometer. Focus was laid on the analysis of field-stressed layers including, inner electrodes and surface precipitates. Additionally, transmission electron microscope investigations (FEI Tecnai F20, FEI, USA) were carried out with samples prepared from virgin and degraded PZT, respectively (lamella preparation: focused ion beam method, FIB).

2.3. Conductive atomic force microscopy (C-AFM)

A NanoScope V Multimode Scanning Probe microscope (Bruker, Germany: formerly Veeco, USA) was employed in an extended C-AFM study with emphasis on the localization of highly conductive paths on and in quenched, degraded layers. This also revealed details on the role of surface precipitates. All scans were conducted using boron-doped diamond coated tips (Pointprobe CONT, NanoWorld, Switzerland). C-AFM measurements were carried out not only on the original surface of highly conductive layers, but also on degraded layers after polishing/grinding steps parallel to the xy-plane and xz-plane, respectively. This yielded information on the depth distribution of conductive paths. Silicon carbide grinding papers (coarseness: #2400 and #4000) and subsequently 1 μm diamond suspension (DiaPro suspension; MD Dac polishing cloth; TegraPol-31 polishing machine) were used for polishing (all products: Struers, Germany).

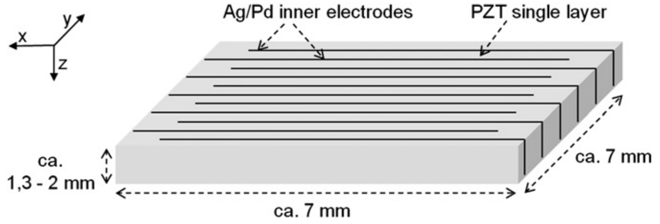

Fig. 1. Sketch of the sample geometry.

In C-AFM measurements on highly conductive materials, the contact resistance between tip and sample surface is frequently the highest serial resistance in the circuit. This contact resistance ($R_{contact}$) depends on the employed tip, the sample and the contact area. Even for a specific tip-sample combination the contact resistance is not necessarily constant, but can depend on the sample topography. Because of these reasons, quantitative interpretation of C-AFM currents (i.e. absolute values) is difficult. Hence, the results in this work are discussed exclusively from a qualitative point of view in terms of high and low currents. During C-AFM measurements, data from all channels (height, friction, current, etc.) may be acquired in either trace (forward run of the tip) or retrace (return path) direction. In this study, current images were measured in both scan directions since, depending on the sample surface, significant differences were partly observed. Accordingly, in several images presented in this paper trace data is marked in red and retrace data in blue color, respectively. For further technical as well as preparative details see Refs. [8,16].

2.4. Laser ablation-inductively coupled plasma-mass spectrometry (LA-ICP-MS)

Distribution of several isotopes (^{46}Ti, ^{48}Ti, ^{90}Zr, ^{92}Zr, ^{105}Pd, ^{106}Pd, ^{108}Pd, ^{107}Ag, ^{109}Ag, ^{142}Nd, ^{144}Nd, ^{146}Nd, ^{206}Pb, ^{207}Pb, ^{208}Pb) was investigated in line scans (spot size 10 μm) of different regions on the surface of both virgin and degraded PZT layers, respectively, using a NWR-213 laser ablation system (New Wave Research, ESI, USA) coupled to a X-Series II ICP-MS System (Thermo Fisher Scientific, Germany). Laser settings and instrument settings of the ICP-MS system were optimized for maximum intensity while maintaining appropriate signal stability by performing a line scan on a certified reference material NIST 612 (determination of the instrumental mass bias). All measurements were then carried out using these optimized settings (Table 1). Owing to the lateral scan-speed of 5 μm/s and the cycle-time required for one scan of all analyzed isotopic masses, a lateral resolution of approx. 1 μm was obtained.

Quantification (estimation) of the silver amount in virgin PZT was done using a mass balance model based on the assumption that the target composition was $Pb_{0.985}Nd_{0.015}Zr_{0.52}Ti_{0.48}O_3$ with natural isotope distribution. Element concentrations were determined from the acquired intensity counts with reference to the three Pb signals and the respective natural isotope abundance.

Table 1
LA-ICP-MS: Instrumental parameters and settings.

Instrumental parameter and settings	Operating conditions
Plasma power [W]	1200
Cooling gas flow [L/min]	13
Auxiliary gas flow [L/min]	0.8
Make up gas flow — Ar [L/min]	0.9
Dwell time per isotope [ms]	10
Laser wavelength [nm]	213
Laser energy [J/cm^2]	12
Laser repetition rate [Hz]	5
Spot size [μm]	10
Scan speed [μm/s]	5
Pulse duration [ns]	5
Carrier gas flow — He [L/min]	0.5